Intermediate-energy proton direct capture populating continuum states

Yu-Kun Ho*
Center of Theoretical Physics, China Center of Advanced Science and Technology (World Laboratory), Beijing, China and Nuclear Science Department, Fudan University, Shanghai, China

Zhu-Shu Yuan
Nuclear Science Department, Fudan University, Shanghai, China
(Received 5 February 1991)

A formalism calculating the cross sections of intermediate-energy proton direct capture populating continuum states has been developed. The transition amplitude includes two terms corresponding to potential-scattering to potential-scattering transitions and potential-scattering to resonance-scattering transitions, respectively. The model is compared with available experimental data of the $^{11}B(p,\gamma_{19})^{12}C$ reaction, and the results show that within the reasonable parameter limit the direct capture mechanism is able to account for a major feature of the measured data, and, in the present case, the contributions from the two terms are of the same order of magnitudes. The physical significance of the results is discussed.

PACS number(s): 25.40.Lw, 24.50.+g

I. INTRODUCTION

About a decade ago, an initial work was reported by Kovash and his collaborators [1] demonstrating strong transitions to highly excited states in ^{12}C and ^{28}Si as they measured the spectra of radiative proton capture reactions in ^{11}B and ^{27}Al at $E_p=40-80$ MeV. For example, pronounced population of the levels at the excitation energies of about 19 MeV in ^{12}C is clearly revealed in the $^{11}B(p,\gamma)$ reaction. The energies of those final states are high enough so that they are in the continuum region of the residual nucleus. It was also pointed out that the transitions have a preference for final states which appear to have a strong single-particle character. This means that there exist positive final state correlations between the intermediate-energy (p,γ) reactions and the $(^3He,d)$ stripping reaction. During that period, most of the theoretical studies [2–7] attributed this phenomenon to the direct capture mechanism. In order to better understand this problem, investigations have been carried out in the following two areas. One is to extend the studies to more nuclides and expand the energy ranges studied. Systematic observations have been carried out for intermediate-energy (p,γ) reactions on targets ^{11}B, ^{15}N, ^{27}Al, ^{39}K, ^{40}Ca populating both bound and continuum states [7–11]. The second area concerned is to explore the similarity for similar single-particle transitions in neighboring nuclear pairs, such as the $^{11}B(p,\gamma)$-$^{12}C(p,\gamma)$ reactions (populating $d_{5/2}$ and $s_{1/2}$ single-particle states), $^{27}Al(p,\gamma)$-$^{28}Si(p,\gamma)$ ($2s_{1/2}, d_{3/2}, f_{7/2}$ states), and $^{16}O(p,\gamma)$-$^{17}F(p,\gamma)$ ($d_{5/2}$ states) [12–14]. All of those studies further confirm that the intermediate-energy proton capture gives priority to final states of larger single-particle fragments. In addition, giant resonance peaks have systematically been observed in the excitation functions populating various final states. It has been suggested that in addition to the direct capture the semidirect capture mechanism should be involved at the energies of the giant dipole resonance (GDR) region.

This paper investigates the direct capture populating continuum states induced by intermediate-energy proton. The motivations of this study are the following.

(1) The calculations performed previously on direct capture should be improved. Those works might be classified into two categories. One [2–4] was to make use of single-particle bound state wave functions instead of the continuum wave functions. This approximation is far from the real situation, and it is not easy to estimate the error caused by the approximation. The other publications [5–7], though, treated the final states as continuum states, but as we will indicate later there exist some problems in connection with the treatment of the wave functions and resonance states. In this paper, we will, based upon the general expressions of the scattering wave functions, present a formalism for direct capture to unbound states by intermediate-energy nucleon.

(2) It is of interest to analyze the measured, especially newly measured, capture data by applying the improved theory to examine the limitation of the direct capture mechanism, and the necessity of involving the semidirect capture in these processes.

(3) The microscopic theory and calculation method of semidirect capture populating continuum states are, perhaps, rather different from that for bound states. One point is that if we evaluate the transition amplitude between continuum state wave functions by using the operator for semidirect capture to bound state, which is localized in space [15], the integral would be extremely small. Thus before we extend the study to the semidirect capture to unbound states, it is good to renew the direct capture theory making it more reliable.

The new formalism for direct capture is presented in

*Mailing address: Nuclear Science Department, Fudan University, Shanghai, China.

Sec. II. Section III contains a full description of the evaluations and results for the $^{11}B(p,\gamma_{19})$ reaction. Finally, the conclusions and brief discussions are summarized in Sec. IV.

II. THEORY

(1) Transition probability. The radiative nucleon direct capture cross section to continuum states in a final state energy interval $E'-E'+dE'$ and solid-angle interval $d\Omega_k$, with the emission of $E1$ radiation, can be written as

$$\frac{d\sigma}{dE'd\Omega_{k'}}=\frac{1}{v}\frac{1}{2(2I+1)}\sum\lambda_{E1}\frac{1}{4\pi}\frac{k'm}{2\pi^2\hbar^2}\ , \tag{1}$$

where

$$\lambda_{E1}=\frac{16\pi}{9}k_\gamma^3\frac{1}{\hbar}|\langle\Psi_f|\bar{e}\mathcal{E}_1Y_{1\nu}|\Psi_i\rangle|^2 \tag{2}$$

is the direct transition probability, v is the incident nucleon velocity, I is the target spin, m is the reduced mass, k' is the nucleon wave number in the final state, k_γ is the photon wave number, $\mathcal{E}_1$ is the radial operator for an electric dipole transition, and Ψ_i and Ψ_f are the initial state and final state wave functions, respectively. We use a superscript prime to designate a quantity belonging to the final state. In Eq. (1), the factor $(1/4\pi)k'm/2\pi^2\hbar^2$ is the final state level density.

(2) The initial state wave function is a plane wave function distorted by the nuclear interaction

$$\Psi_i=\sum_{l=0}\sum_{j=l-1/2}^{l+1/2}\sum_{J=|j-I|}^{j+I}\sqrt{4\pi}(2l+1)\frac{\mathrm{Re}\langle U_{lj}^{+J}(kr)\rangle}{kr}\times C_{l0\,1/2\,\mu}^{j\mu}C_{j\mu Im_I}^{JM}\mathcal{Y}_{ljI}^{JM}\ , \tag{3}$$

where k is the incident nucleon wave number, C's are Clebsch-Gordan coefficients, and $\mathcal{Y}_{ljI}^{JM}$ is the channel wave function consisting of the intrinsic ground state wave function of the target nucleus coupled to the nucleon wave function of angular momentum (l,j) to give total spin J and projection M. We use Re and Im to designate the real and imaginary parts. Equation (3) is readily obtained [16] by replacing the spherical Bessel function $j_l(kr)$ in the partial wave expansion of the plane wave by the optical model potential-scattering wave function $\mathrm{Re}\langle U_{lj}^{+J}(kr)\rangle/kr$. For the direct capture, only the potential-scattering wave in the initial state should be taken into account.

(3) Final state wave function. By making use of the identity

$$e^{ik'r}=\sum_{l'=0}\sum_{m_{l'}=-l'}^{l'}4\pi i^{l'}j_{l'}(k'r)Y_{l'm_{l'}}^*(k')Y_{l'm_{l'}}(r)\ , \tag{4}$$

the final state wave function is obtained

$$\Psi_f=\sum_{l'=0}\sum_{m_{l'}=-l'}^{l'}\sum_{j'=l'+1/2}\sum_{J'=|j'-I|}^{j'+I}4\pi i^{l'}\frac{U_{l'j'}^{+J'}(k'r)}{k'r}Y_{l'm_{l'}}^*(k')C_{l'm_{l'}\,1/2\,\mu}^{j'm_{j'}}C_{j'm_{j'}Im_I}^{J'M'}\mathcal{Y}_{l'j'I}^{J'M'}\ , \tag{5}$$

where [17]

$$U_{l'j'}^{+J'}(k',r)=\mathrm{Re}\langle U_{l'j'}^{+J'}(k'r)\rangle+\frac{1}{2}\sum_\lambda\frac{\Gamma_{p\lambda}}{E_\lambda-E'-i\Gamma_\lambda/2}N_{l'j'}(k'r)\ , \tag{6}$$

and

$$N_{l'j'}(k'r)=\frac{\mathrm{Im}\langle U_{l'j'}^{+J'}(k'r)\rangle}{\langle K_{l'j'}^{J'}\rangle}\ , \tag{7}$$

$\langle K_{l'j'}^{J'}\rangle$ is the reactance matrix element calculated by the optical model, E_λ, Γ_λ, and $\Gamma_{p\lambda}$ denote the nearby resonance parameters. The first term in Eq. (6) is the potential-scattering wave, and the second term is the resonance-scattering wave.

(4) Direct capture cross section. Inserting Eqs. (3) and (5) into Eq. (1), and using the identity

$$\langle\mathcal{Y}_{l'j'I}^{J'M'}|Y_{1\nu}|\mathcal{Y}_{ljI}^{JM}\rangle=C_{JM1\nu}^{J'M'}(-1)^{I+1/2-l-j-j'-J'}C_{l010}^{l'0}\times\left[\frac{3}{4\pi}(2l+1)(2j+1)(2J+1)(2j'+1)\right]^{1/2}W(jJj'J',I1)W(ljl'j',\tfrac{1}{2}1)\ , \tag{8}$$

and

$$\sum|C_{l0\,1/2\,\mu}^{j\mu}C_{j\mu Im_I}^{JM}C_{l'm_{l'}\,1/2\,\mu'}^{j'm_{j'}}C_{j'm_{j'}Im_I'}^{J'M'}C_{JM1\nu}^{J'M'}|^2=\frac{2J'+1}{2l+1}\ , \tag{9}$$

the differential cross section of direct capture populating continuum states is obtained

$$\frac{d\sigma}{dE'}=\frac{32}{3}\frac{k_\gamma^3m}{vk^2k'\hbar^3}\sum\frac{2J+1}{2(2I+1)}\langle ljJ|D_I|l'j'J'\rangle(2J'+1)\bar{e}^2\left|\int\mathcal{E}_1U_{l'j'}^{+J'}(k'r)\mathrm{Re}\langle U_{lj}^{+J}(kr)\rangle dr\right|^2\ , \tag{10}$$

where

$$\langle ljJ|D_I|l'j'J'\rangle=(2l+1)(2j+1)(2j'+1)\left[C^{l'0}_{l010}W(jJj'J',I1)W(ljl'j',\tfrac{1}{2}1)\right]^2 . \tag{11}$$

Using Eq. (6), the radial integral in Eq. (10) is calculated to contain three terms

$$\left|\int \mathcal{E}_1 \mathrm{Re}\langle U^{+J'}_{l'j'}(k'r)\rangle \mathrm{Re}\langle U^{+J}_{lj}(kr)\rangle dr\right|^2+\frac{1}{4}\left|\sum_\lambda \frac{\Gamma_{p\lambda}}{E_\lambda-E'-i\Gamma_\lambda/2}\right|^2\left|\int \mathcal{E}_1 N_{l'j'}(k'r)\mathrm{Re}\langle U^{+J}_{lj}(kr)\rangle dr\right|^2$$
$$+\mathrm{Re}\left[\sum_\lambda \frac{\Gamma_{p\lambda}}{E_\lambda-E'-i\Gamma_\lambda/2}\int \mathcal{E}_1 N_{l'j'}(k'r)\mathrm{Re}\langle U^{+J}_{lj}(kr)\rangle dr\right]^*\left[\int \mathcal{E}_1 \mathrm{Re}\langle U^{+J'}_{l'j'}(k'r)\rangle \mathrm{Re}\langle U^{+J}_{lj}(kr)\rangle dr\right] \tag{12}$$

corresponding to potential-scattering to potential-scattering transitions, potential-scattering to resonance-scattering transitions, and their interference, respectively. The last two terms make a contribution to the fine resonance structure appearing in the gamma-ray energy spectra. We note that the previous calculations [5–7] included only the first term in Eq. (12).

(5) Cross section averaged over the final state energy. In the case that the final states are too close to resolve experimentally, the measured data are the averaged cross sections over the final state energy

$$\left\langle \frac{d\sigma}{dE'}\right\rangle_{E'}=\frac{1}{\Delta E}\int_{E'-\Delta E/2}^{E'+\Delta E/2}\frac{d\sigma}{dE'}dE' , \tag{13}$$

where ΔE is an energy space over which the average is performed. Using the identity

$$\left\langle\left|\sum \frac{\Gamma_{p\lambda}}{E_\lambda-E'-i\Gamma_\lambda/2}\right|^2\right\rangle=\frac{T_{l'j'}T_{l'j'}}{T^{J'}}W^{J'}_{l'j'l'j'} , \tag{14}$$

where $T^{J'}$ and $T_{l'j'}$ are the total and nucleon partial transmission coefficients, respectively, $W_{l'j'l'j'}$ are the width fluctuation correlation factors, then the averaged direct capture cross section is

$$\left\langle \frac{d\sigma}{dE'}\right\rangle_{E'}=\frac{32}{3}\frac{k_\gamma^3 m}{vk^2k'\hbar^3}\sum\frac{2J+1}{2(2I+1)}\langle ljJ|D_I|l'j'J'\rangle(2J'+1)\bar{e}^2$$
$$\times\left[\left|\int \mathcal{E}_1\mathrm{Re}\langle U^{+J'}_{l'j'}(k'r)\rangle\mathrm{Re}\langle U^{+J}_{lj}(kr)\rangle dr\right|^2\right.$$
$$\left.+\frac{1}{4}\frac{T_{l'j'}T_{l'j'}}{T^{J'}}W^{J'}_{l'j'l'j'}\left|\int \mathcal{E}_1 N_{l'j'}(k'r)\mathrm{Re}\langle U^{+J}_{lj}(kr)\rangle dr\right|^2\right] . \tag{15}$$

We note that all quantities in Eq. (15) can be evaluated by the optical model. In contrast to Eq. (12), Eq. (15) contains no interference term. This feature may be understood in the same way as calculating the averaged nucleon scattering cross sections, where there is no interference term between the shape elastic and compound elastic scattering amplitude. The first term in Eq. (15) corresponds to a transition to the potential-scattering state, where no compound nucleus is formed, whereas the second term refers to a transition to the compound elastic scattering state, where the factor $T_{l'j'}T_{l'j'}/T^{J'}$ represents the processes of formation and decay of the compound nucleus in the final states.

III. COMPARISON WITH EXPERIMENT

In this section, we will discuss three questions, namely, the evaluation of the radial integral for transition between continuum states, the non-long-wavelength approximation to the electric multipole transition operator, and a comparison of the results of direct capture calculations to the measured data for the $^{11}\mathrm{B}(p,\gamma_{19})^{12}\mathrm{C}$ reaction.

(1) As one evaluates the transition matrix elements in Eqs. (10) and (15), the most troublesome problem is the calculation of the radial integrals. Since both the initial state and final state wave functions are continuum in nature, and the transition operator is also not confined in space, it is impractical to integrate directly. We have utilized the contour integration method developed by Vincent and Fortune [18,6,7]. In this technique, a separation radius R_m is set up to break the integral up into two parts

$$\int_0^\infty=\int_0^{R_m}+\int_{R_m}^\infty . \tag{16}$$

The first integral of Eq. (16) can be evaluated by direct numerical integration. The calculation of the second integral may be performed instead by integrating along the contours C_2-C_+ or C_1-C_- as shown in Fig. 1. Provided R_m is chosen such that $k'R_m\gg1$, then the terms in the integrand decay exponentially along either the imaginary axis C_2 or C_1, and rapid convergence of the integral is obtained. In the calculations of the $^{11}\mathrm{B}(p,\gamma_{19})$ reaction, we have found that convergence is achieved with $R_m=30$ fm and $Y_m=20$ fm, and the whole integral is independent of the specific choice of R_m.

(2) The standard electric multipole transition operator [19] has been applied in the present calculations

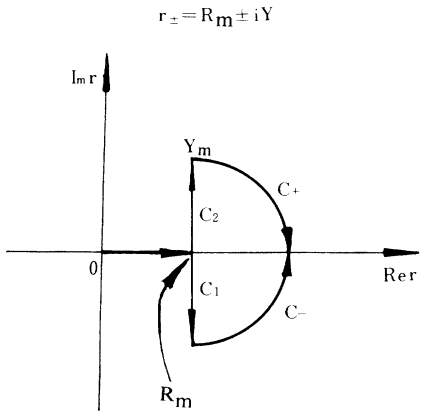

FIG. 1. The contour integrations along the path C_2-C_+ or C_1-C_- were used to calculate the radial integral.

$$\mathcal{E}_L=\frac{2L+1}{(L+1)k_\gamma^L}[(L+1)j_L(k_\gamma r)-k_\gamma r j_{L+1}(k_\gamma r)] . \tag{17}$$

The frequently used long-wavelength approximation (r^L) is certainly improper for calculating transition amplitudes between continuum states. We use the effective charge to cover the target recoil effect. The corrections arising from the magnetic moment current and spin-orbit coupling current are expected to be small, typically yielding a 5% correction to the cross section [20], and ignored here. The possible contributions from the exchange current [3,24] were also ignored in Eq. (17).

(3) Both the experimental and theoretical studies for the $^{11}B(p,\gamma_{19})$ reaction were quite extensively performed previously [1,5–7]. Weller *et al.* [7] attributed the strength bump in the 19 MeV region of ^{12}C in the spectra to a superposition of three sharp peaks at energies of 18.43, 19.65, and 20.68 MeV. It seems, however, that the experimental resolution was not sufficient to fully identify the fine structure. In fact, quite a lot of discrete resonance states have been established experimentally in this energy region [21]. Thus we utilize Eq. (15) to calculate the energy-averaged direct capture cross section. The experimental data are taken from Ref. [7], and the bump width in the 19 MeV region of the spectra is taken to be 2.5 MeV.

The potential parameters listed in Table I were used to calculate the scattering wave functions and S matrix elements of the initial state and final state, respectively [23]. The parameters are based upon the potentials given in Ref. [7]. The potential for the final state was adjusted to place the peak of the $d_{5/2}$ partial wave transmission coefficient at 19.5 MeV. The potential to calculate the initial state was adjusted according to both the proton scattering data and the pattern of the $^{11}B(p,\gamma_{19})$ excitation function. Figure 2 shows the contributions to the excitation function of partial wave $f_{7/2}$-$d_{5/2}$ transition from the two terms in Eq. (15), respectively, and the sum. It can be seen that the two contributions are of the same order of magnitudes. To explain this result, we note that the nucleon energy corresponding to the final state of the

TABLE I. Optical model parameter for $^{11}B(p,\gamma_{19})$. The reader is referred to Ref. [22] for the nomenclature of the parameters.

	Initial state	Final state
V_0 (MeV)	50.0	52.4
W_s (MeV)	3.38	0.4
V_{s0} (MeV)	7.79	6.64
r_0 (fm)	1.12	1.23
r_s (fm)	1.30	1.16
r_{s0} (fm)	0.98	1.03
r_c (fm)	1.29	1.10
a_0 (fm)	0.63	0.66
a_s (fm)	1.01	0.83
a_{s0} (fm)	0.57	0.66

$^{11}B(p,\gamma_{19})$ reaction is about 3.5 MeV. In this case, only one of the inelastic channels is opened. Thus the compound elastic scattering amplitude in the external region is relatively strong, and the contributions to the cross sections from the potential-compound transition would be comparable to that from the potential-potential transition. With an increase of the excitation energy in the final state, the number of opened channels will increase and the fraction of compound nucleus processes will continue to decrease. Figure 3 exhibits a comparison of the measured data and the results of direct capture calculations for the $^{11}B(p,\gamma_{19})$ excitation function. Three transitions for the incident channels $(l,j)=f_{7/2}$, $f_{5/2}$, and $p_{3/2}$ going to the continuum final states having $(l',j')=d_{5/2}$ are presented. In addition, the calculated results of Ref. [7] are also included here for comparison. We note that among the three partial wave transitions, the contribution from the $f_{7/2}$-$d_{5/2}$ transition is the dominant one, and the calculated total direct capture cross sections may account for the major feature of the measured data, such as the order of magnitude of the cross sections and the behavior of the excitation function via the incident ener-

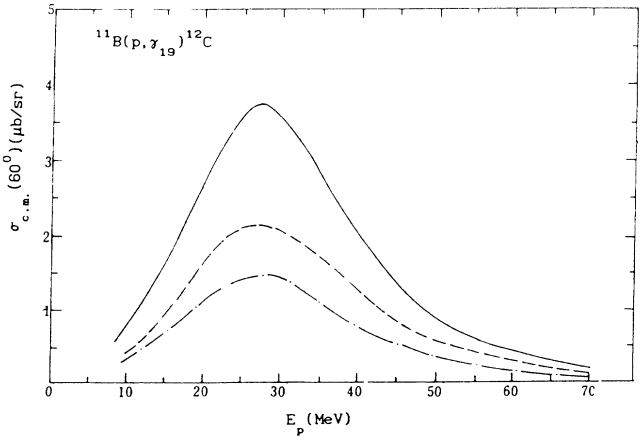

FIG. 2. The calculated $^{11}B(p,\gamma_{19})$ excitation function of the transition from the partial wave $f_{7/2}$ to the final states of $d_{5/2}$. The dashed and dash-dotted lines represent the contributions from the first and second terms of Eq. (15), respectively. The solid line gives the sum.

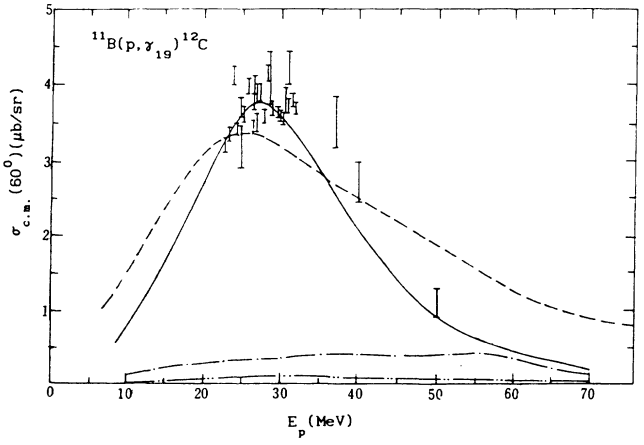

FIG. 3. A comparison of the measured data and the results of direct capture calculations for the $^{11}B(p,\gamma_{19})$ excitation function. The measured data are taken from Ref. [7]. The solid, dash-dotted, and dash-dot-dotted lines represent the contributions from the partial wave transitions to the $d_{5/2}$ final state from the incident channels $f_{7/2}$, $f_{5/2}$, and $p_{3/2}$, respectively. The dashed line gives the calculated results of Weller *et al.* [7].

gy. We did not compare the data for angular distribution of the cross sections and analyzing power, which are insensitive to the reaction mechanism [7].

IV. CONCLUSIONS AND BRIEF DISCUSSIONS

This paper investigated the direct capture transition to continuum states. Based upon a unified description of the initial state and final state wave functions [Eqs. (3) and (5)], the formalism calculating the direct capture cross sections populating unbound states is presented, which contains three terms corresponding to the potential-scattering to potential-scattering transition, potential-scattering to resonance-scattering transition, and their interference, respectively [Eqs. (10) and (12)].

Equation (15) is the energy-averaged direct capture cross section over the final state energy. All quantities in this equation may be calculated with the optical model. In contrast to Eq. (12), Eq. (15) contains no interference term. As the nucleon energy with regard to the final state is relatively close to the nucleon binding energy, the amplitude of the relevant compound elastic scattering wave in the external region is comparable to that of the shape elastic scattering wave, then the contributions from the two terms in Eq. (15) are of the same order of magnitudes.

The calculation results of the $^{11}B(p,\gamma_{19})$ reaction indicate that the direct capture model is able to account for the major feature of the measured data in the present case. More calculations and comparisons on various examples are needed to examine the capability of the direct capture model before we may draw any definite conclusion about the necessity of including the semidirect capture mechanism in the capture transitions to continuum states. However, at least, the results of the $^{11}B(p,\gamma_{19})$ reaction demonstrate that there exists a difference between the direct capture transition to unbound states and that to bound states. The former may account for a considerable part of the total capture cross sections, whereas the latter is normally far below the contribution from the semidirect capture near the GDR energy region.

This work was supported partly by the International Atomic Energy Agency under Contract No. 5232/R2/RB.

[1] M. A. Kovash, S. L. Blatt, R. N. Boyd, T. R. Donoghue, H. J. Hausman, and A. Bacher, Phys. Rev. Lett. **42**, 700 (1979).
[2] J. T. Londergan and L. D. Ludeking, Phys. Rev. C **25**, 1722 (1982).
[3] S. F. Tsai and J. T. Londergan, Phys. Rev. Lett. **43**, 576 (1979).
[4] L. G. Arnold, Phys. Rev. Lett. **42**, 1253 (1979).
[5] Dean Halderson and R. J. Philpott, Phys. Rev. Lett. **46**, 100 (1981).
[6] R. J. Philpott and Dean Halderson, Nucl. Phys. **A375**, 169 (1982).
[7] H. R. Weller *et al.*, Phys. Rev. C **25**, 2921 (1982).
[8] M. Nomachi, T. Shibata, K. Okada, T. Motobayashi, F. Ohtani, and H. Ejiri, Phys. Rev. C **9**, 242 (1985).
[9] A. Anghinolfi, P. Corvisiero, G. Ricco, M. Taiuti, and A. Zucchiatti, Nucl. Phys. **A399**, 66 (1983).
[10] D. Dowel, G. Feldman, K. Snover, A. Sandorfi, and R. O. Owens, Phys. Rev. Lett. **50**, 1191 (1983).
[11] J. D. Kalen, H. J. Hausman, A. Abduljalil, W. Kim, D. G. Marchlenski, J. P. McDermott, T. W. Rackers, S. L. Blatt, M. A. Kovash, and A. D. Bacher, Phys. Rev. C **39**, 340 (1989).
[12] S. L. Blatt, in *Capture Gamma-Ray Spectroscopy and Related Topics (Holiday Inn—World's Fair, Knoxville, Tennessee)*, Proceedings of the Fifth International Symposium on Capture Gamma-Ray Spectroscopy and Related Topics, edited by S. Raman, AIP Conf. Proc. No. 125 (AIP, New York, 1984), p. 570.
[13] S. L. Blatt, H. J. Hausman, L. G. Arnold, R. G. Seyler, R. N. Boyd, T. R. Donoghue, P. Koncz, M. A. Kovash, A. D. Bacher, and C. C. Foster, Phys. Rev. C **30**, 423 (1984).
[14] T. W. Rackers, S. L. Blatt, T. R. Donoghue, H. J. Hausman, J. Kalen, W. Kim, D. G. Marchlenski, M. Wiescher, M. A. Kovash, and A. D. Bacher, Phys. Rev. C **37**, 1759 (1988).
[15] I. Bergqvist, in *Neutron Radiative Capture*, edited by R. E. Chrien (Pergamon, New York, 1984), p. 33.
[16] Y. K. Ho and M. A. Lone, Nucl. Phys. **A406**, 17 (1983).
[17] Y. K. Ho and M. A. Lone, Nucl. Phys. **A406**, 1 (1983).
[18] C. M. Vincent and H. T. Fortune, Phys. Rev. C **2**, 782 (1970).
[19] H. T. Rose and D. M. Brink, Rev. Mod. Phys. **39**, 306 (1967).
[20] J. M. Lafferty and S. R. Cotanch, Nucl. Phys. **A373**, 363 (1982).
[21] F. Ajzenberg-Selove, Nucl. Phys. **A433**, 1 (1985).
[22] O. Karban, J. Lowe, P. D. Greaves, and V. Hnizdo, Nucl.

Phys. **A133**, 255 (1969).

[23] As it stands, different potentials were used for levels at different excitation energies of the same nuclide. This technique has been used frequently in the literature. As indicated by Noble and his collaborators [Phys. Rev. C **17**, 2151 (1978); **19**, 276 (1981)], a violation of the orthogonality of the initial and final state wave functions (the formalism used here is not gauge invariant) may appreciably change the overlap integral in transition amplitude. A judgment for this treatment is a long-standing problem of shell model, and it is beyond the scope of this paper.

[24] M. Gari and H. Hebach, Phys. Rep. **72**, 1 (1981).